EPJ Web of Conferences **86**, 00013 (2015)
DOI: 10.1051/epjconf/ 20158600013

Effect of shell structure on neutron multiplicity of fissioning systems ^{220,222,224}Th nuclei

Savi Goyal[1,a], S. Mandal[1], Akhil Jhingan[2], P. Sugathan[2], Santanu Pal[3], B. R. Behera[4], K. S. Golda[2], Hardev Singh[5], Sunil Kalkal[1], Varinderjit Singh[4], Ritika Garg[1], Davinder Siwal[1], Maninder Kaur[4], Mansi Saxena[1], Suresh Kumar[1], S.Verma[1], M. Gupta[6], Subinit Roy[7] and R. Singh[8]

[1]*Department of Physics and Astrophysics, University of Delhi, Delhi, INDIA*
[2]*Inter University Accelerator Centre, Aruna Asaf Ali Marg, New Delhi, INDIA*
[3] *CS-6/1, Golf Green, Kolkata. Formerly with Variable Energy Cyclotron Centre, Kolkata, INDIA*
[4]*Department of Physics, Panjab University, Chandigarh, INDIA*
[5]*Department of Physics, Kurukshetra University, Kurukshetra, INDIA*
[6]*Manipal Centre for Natural Sciences, Manipal University, Manipal, INDIA*
[7]*Saha Institute of Nuclear Physics, Kolkata, INDIA*
[8]*Amity Institute of Nuclear Science and Technology, Noida, INDIA*

Abstract. The pre- and post-scission neutron multiplicities have been extracted for the ^{220,222,224}Th nuclei for the excitation energy range of 40 MeV to 64 MeV using the National Array of Neutron Detectors (NAND). The Th isotopes are populated from the fusion reaction of ^{16}O+^{204,206,208}Pb systems in order to investigate the dynamics of fusion-fission reactions using the neutron multiplicity as a probe. The theoretical calculations were performed using the Bohr-Wheeler fission width as well as the dissipative dynamical fission width from Kramers prescription. It is observed that the Bohr-Wheeler fission width underestimates the pre-scission yields to a large extent. A large amount of dissipation is required in the Kramers width to fit the observed pre-scission neutron multiplicities.

1 Introduction

Considerable progress has been made in the last few years in the understanding of the fission of a highly excited compound nucleus formed in heavy-ion reactions, both experimentally and theoretically. Large volumes of experiments have been performed using a number of experimental probes to investigate the several aspects of the dynamics of the fusion-fission reactions. The particles emitted during the fission process, and in particular the pre-scission ones represent a powerful tool to investigate the fission dynamics [1-4]. These studies have resulted in the interesting observation of the substantially higher yield of pre-scission charged particles [1], neutrons [2-3] and gamma rays [4] than those predicted by the standard statistical model of fission [5]. These measurements represent the evidence of the effects of nuclear viscosity in the fission process.

Neutron emission is one of the dominant decay channels in heavy ion induced fusion-fission reactions. The large excess of neutrons which are emitted before the nucleus undergoes fission immediately points to a slowing down of the fission process compared with the statistical model fission rate as given by Bohr and Wheeler [6]. It is interpreted as arising from the dynamical effects in the fission decay process. Investigation also shows shell effects play a crucial role in investigating the fusion-fission dynamics. A shell-closed nucleus has a high binding energy, which lowers the probability of particle emission and on the same time shell closed nuclei has high fission barrier, which enhances the probability of particle emission [7]. Therefore it will be interesting to study the shell effects of projectile and target on the neutron multiplicity from the fissioning systems. In the present paper, we are reporting the study of pre- and post-scission neutron multiplicities and the shell effects for ^{16}O + ^{204,206,208}Pb systems at energies near and above the Coulomb barrier. We also give the nature and strength of nuclear viscosity by comparing the data with the dynamical models.

2 Experimental Set-up

The experiment was carried out at Inter University Accelerator Centre (IUAC) using the ^{16}O pulsed beam (repetition rate-250 nsec) of energies from 90 MeV to 120 MeV from the Pelletron and the energy booster LINAC using the neutron detector set-up known as National Array of Neutron Detectors (NAND). The self-supporting isotopically enriched ^{204,206,208}Pb targets [8] of thickness~1.5 mg/cm^2 were placed at the centre of the chamber of thickness 3 mm and diameter 60 cm. The

[a] Corresponding author: savi.november@gmail.com

^{220,222,224}Th was populated as the compound nuclei at the excitation energies ranging from 40 MeV to 64 MeV. For the detection of fission fragments, a pair of Multi-Wire Proportional Counters (MWPCs) of active area 20 cm x 10 cm were placed inside the chamber at the folding angles calculated using Viola systematics [9] at a distance of 19.6 cm and 21 cm respectively from the target. Two Silicon Surface Barrier Detectors (SSBD) were also placed at ± 16° w.r.t the beam direction inside the scattering chamber to monitor the movement of the beam spot. For the detection of neutron, 16 NE213 organic liquid scintillators of dimensions 5"x5" were placed in a cylindrical manner around the scattering chamber at distance of 2 m from the target position. A schematic diagram of the scattering chamber and arrangement of the neutron detectors around it is shown in Fig.1.

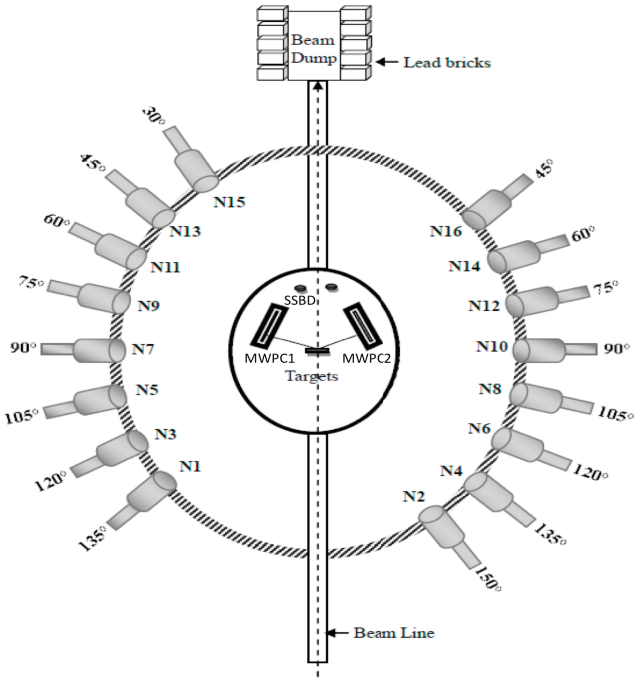

Figure 1. A schematic of the NAND set-up.

To minimize the contribution from the background sources, the beam was dumped 4 m downstream from the target and was well shielded with lead bricks and borated paraffin. The event trigger of the data acquisition system was generated by the OR of the cathode signals of the two fission detectors ANDed with the RF of the beam pulse. The n-γ discrimination was made by using the Time of Flight (TOF) and pulse shape discrimination method based on zero crossover technique [10]. The TOF of neutrons were converted into neutron energy by considering the prompt position of gamma in the TOF spectrum as the reference time. The efficiency correction for the neutron detectors was done using the statistical Monte-Carlo code MODEFF [11].

3 Data analysis and results

To extract the pre- and post-scission components of the neutron multiplicities per fission, the energy spectrum of all the neutron detectors were fitted simultaneously by using a multiple source (pre-scission component is assumed to be from the CN and the post-scission from the two fully accelerated fission fragments) least square fitting procedure using the Watt expression [12] given as

$$\frac{d^2M_n}{dE_n d\Omega_n} = \sum_{i=1}^{3} \frac{M_n^i \sqrt{E_n}}{2(\pi T_i)^{3/2}} \exp\left[-\frac{E_n - 2\sqrt{\varepsilon_i E_n}\cos\theta_i + \varepsilon_i}{T_i}\right]$$

where, the running index i corresponds to all moving sources of the neutron emission that is compound nucleus and the fission fragments. E_n is the laboratory energy of the neutron and E_i, T_i, M_{ni} represents kinetic energy, temperature and multiplicity of each neutron emission source. A_i is mass of each neutron source and θ_i represents the relative angle between neutron direction and the source direction. The kinetic energies of the fission fragments were calculated using the Viola [9] systematics, for symmetric fission. In order to find out the relative angle between the source direction and the neutron direction, the angular acceptance of both the neutron detectors and the fission detectors were taken into account. The post scission neutron multiplicity and the temperature (T_{post}) were assumed to be same for both the fission fragments. Hence the total neutron multiplicity is given as $M_{tot} = M_{pre} + 2*M_{post}$. Here M_{pre} is the pre-scission neutron multiplicity and M_{post} is the post-scission neutron multiplicity. The fits for the data were obtained using χ^2 minimization with M_{pre}, M_{post}, T_{pre} and T_{post} as free parameters.Fig. 2 shows the fits to the double differential neutron multiplicity spectra at various angles for ^{16}O+ ^{208}Pb reaction at 99.4 MeV. It shows that at angle around θ_{nf} = 90°, the contribution of pre-scission dominates whereas at angle 0° (or 180°), spectra are dominated by the contribution from the post-scission component.

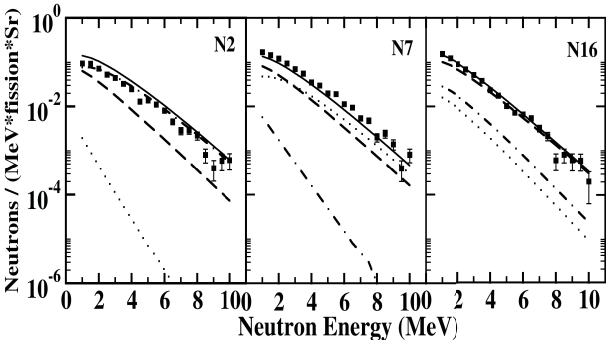

Figure 2. Neutron multiplicity spectra (solid squares) for the ^{16}O+^{208}Pb reaction at E_{lab} = 99.4 MeV along with the fits for the pre-scission (dotted-curve) and post-scission from fragment 1 (dot-dashed) and fragment 2 (dashed curve). The solid line represents the total contribution.

Fig. 3 shows the calculated excitation function of M_{pre} and the excitation function for M_{post} for different compound nuclei is given in Fig 4. The M_{pre} and M_{post} don't show any remarkable dependence on the shell effects of the system. M_{pre} is found to be increasing with the increasing excitation energy. M_{post} does not show any noticeable dependence on excitation energy of the CN as well, as most of the excess in excitation energy of CN is

being carried away by the pre-scission neutrons. The major contribution to the increase in total neutron multiplicity with excitation energy of the CN comes from the pre-scission neutrons, as post-scission component is not having any remarkable dependence on the excitation energy of the CN.

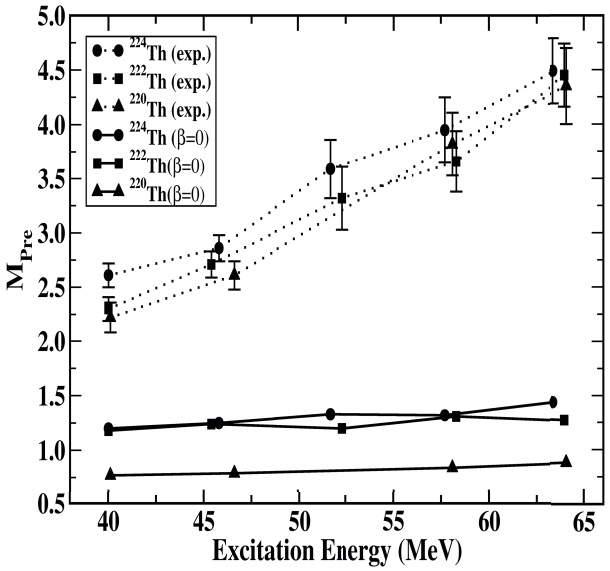

Figure 3. Experimental value of M_{pre} as a function of excitation energy along with the statistical model calculations (β=0). The lines are drawn to guide the eye.

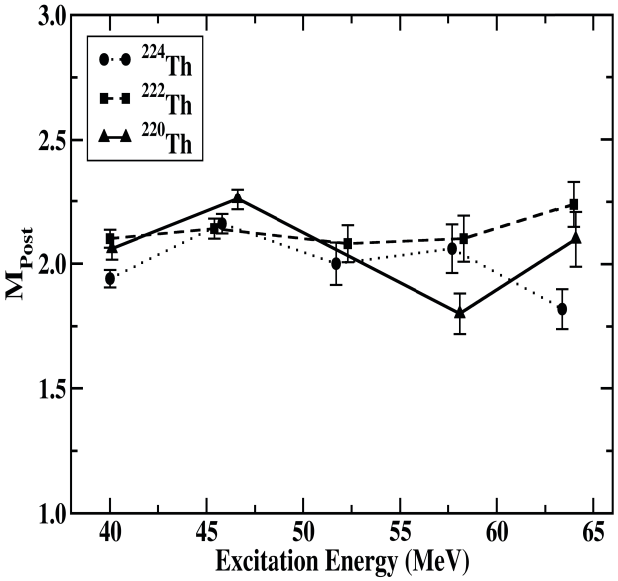

Figure 4. Experimental value of M_{post} as a function of excitation energy. The lines are drawn to guide the eye.

4 Statistical Model Analysis

The experimentally measured values of pre- and post-scission neutron multiplicities were compared with the statistical model predictions. In the statistical model calculations, in addition to fission, emission of light particles (neutrons, protons and α) and GDR γ rays were considered as possible decay channels for an excited nucleus. The light particle and GDR γ-ray partial widths were obtained from the Weisskopf formula [13]. In the present work fission width is taken from the work of Kramers [14]. The Kramers fission width corresponding to the stationary regime in a dissipative decay of excited compound nucleus is given as:

$$\Gamma_K = \frac{\hbar\omega_g}{2\pi}\Gamma_{BW}\left[\sqrt{1+\left(\frac{\beta}{2\omega_s}\right)^2}-\frac{\beta}{2\omega_s}\right] \qquad (1)$$

where β is the reduced dissipation coefficient, ω_g and ω_s are the frequencies of the harmonic oscillator potentials which have same curvatures as the LDM nuclear potential at the ground-state and saddle configuration, respectively. Γ_{BW} is the above equation is the transition-state fission width due to Bohr and Wheeler [14] and is given as

$$\Gamma_{BW} = \frac{1}{2\pi\rho_g(E_i)}\int_0^{E_i-V_B}\rho_s(E_i-V_B-\varepsilon)d\varepsilon$$

where ρ_g is the level density at the initial state and ρ_s is the level density at the saddle point. V_B denotes the fission barrier. The nuclear potential is obtained as a function of elongation using the finite range liquid drop model (FRLDM) [15].

In a dissipative dynamical model of nuclear fission, the stationary value of fission width (Eq. 1) is reached after a build up or a transient time period τ_f [16]. The incorporation of build up time parameterizes the dynamical fission width as [17]

$$\Gamma_f(t) = \left[1-\exp\left(-2.3t/\tau_f\right)\right]\Gamma_K .$$

In the above definition of the fission width, fission is considered to have taken place when the CN crosses the saddle deformation. During transition from saddle-to-scission, the CN can emit further neutrons, which would contribute to the pre-scission multiplicity. The saddle-to-scission time interval is given as [18]

$$\tau_{ssc} = \left[\tau^0_{ssc}\left(1+\gamma^2\right)^{1/2}+\gamma\right]$$

where τ^0_{ssc} is the non-dissipative saddle-to-scission time interval and its value is taken from [19]. The multiplicity of neutrons emitted from the fission fragments (M_{post}) assuming symmetric fission has also been calculated.

An important parameter for the particle and γ decay widths is the level density parameter, which is taken from the work of Ignatyuk *et al*. [20]. It incorporates the nuclear structure at low excitation energy and goes smoothly to the liquid drop behavior at high excitation energy.

The statistical model calculations were performed with $\beta = 0$ in Eq. (1) which reduces the Kramers fission width to the Bohr-Wheeler transition state fission width. The calculated excitation function for M_{pre} is compared with the experimental values in Fig. 3. It is observed that experimental pre-scission neutron multiplicities are under-predicted by the statistical model predictions for all the cases.

Pre-scission multiplicities are next calculated by varying the values of β in the Kramers fission width. The fission width decreases with increasing value of β resulting in larger value of M_{pre} values. The value for which the calculated value of M_{pre} matches the experimental value is taken as the best-fit β value for a given system. Fig. 5 shows the variation of the best-fit values of β with the experimental M_{pre} for different compound nuclei with the increasing excitation energies. It is observed that as the value of M_{pre} (excitation energy) increases, the dissipation strength also increases for all the systems. It can also be seen (Fig. 5), the magnitude of dissipation strength required to reproduce the experimentally measured value of M_{pre}, at each excitation energy is higher for ^{220}Th compared with the corresponding ^{222,224}Th nuclei. This trend can be due to the possible shell effects of the system.

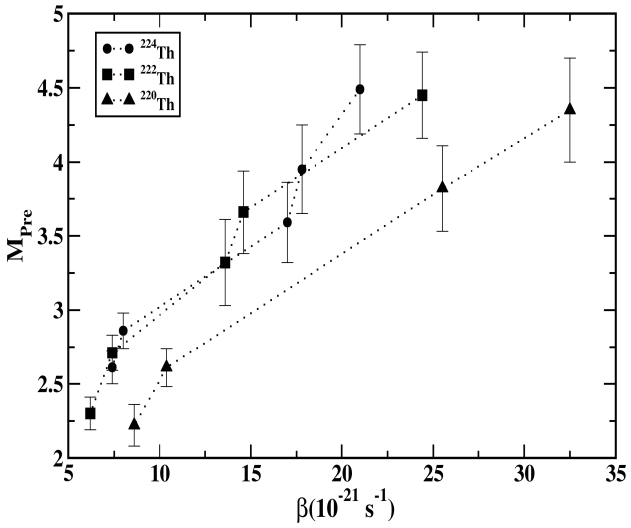

Figure 5. Variation of M_{pre} with β for different systems. The lines are drawn to guide the eye.

5 Summary

Pre- and post-scission neutron multiplicities have been measured for the ^{16}O+^{204,206,208}Pb reactions at various excitation energies. The experimentally measured neutron multiplicities increase with the excitation energy and were compared with the statistical model predictions using the Kramers fission width. The present result shows that a dissipative fission dynamics is essential to explain the measured multiplicities of pre-scission neutrons. It was observed that the dissipation strength increases with the excitation energy of the CN.

Acknowledgments

The author would like to thank the Pelletron and LINAC groups of IUAC, New Delhi, for providing excellent quality of beam throughout the experiment. We are also thankful to Prof. Hans Wollersheim for providing us the enriched ^{204}Pb target. One of the author (SG) is also thankful to UGC for providing us the financial support as fellowship.

References

1. J. P. Lestone *et al*., Phys. Rev. Lett. **67**, 1078 (1991).
2. D. J. Hinde *et al*., Nucl. Phys. A **452**, 550 (1986).
3. H. Rossner *et al*., Phys. Rev. C **45**, 719 (1992).
4. M. Thoennessen *et al*., Phys. Rev. Lett. **59**, 2860 (1987).
5. A. Gavron *et al*., Phys. Rev. Lett. **47**, 1255 (1981), erratum: **48**, 835 (1982).
6. N. Bohr and J. A. Wheeler, Phys. Rev. **56**, 426 (1939).
7. Y. E. Wei, Chin. Phys. Lett., Vol. **20**, No.4, 482 (2003).
8. Savi Goyal *et al.*, Submitted to Nucl. Instr. and Methods (2014).
9. V. E. Viola *et al.*, Phys. Rev. C **31**, 1550 (1985).
10. S. Venkataramanan *et al*., Nucl. Instr. and Meth. in Phys. Research A **596**, 248 (2008).
11. R. A. Cecil *et al.*, Nucl. Instrum. Methods **161**, 439 (1979).
12. D. Hilscher *et al.*, Phys. Rev. C **20**, 576 (1979).
13. F. Puhlhofer, Nucl. Phys. A **280**, 267 (1977).
14. Jhilam Sadhukhan *et al.*, Phys. Rev. C **79** (2009) 064606.
15. A. J. Sierk, Phys. Rev. C **33**, 2039 (1986).
16. P. Grange *et al*., Phys. Rev. C **27**, 2063 (1983).
17. K. H. Bhatt *et al.*, Phys. Rev. C **33**, 954 (1986).
18. H. Hofmann *et al*., Phys. Lett. B **122**, 117 (1983).
19. P. Grange *et al*., Phys. Rev. C **34**, 209 (1986).
20. A. V. Ignatyuk *et al*., Yad. Fiz. **21**, 485 (1975) [Sov. J. Nucl. Phys. **21**, 255 (1975)].